

# Effective and Feasible Photocatalytic Degradation of Janus Green B dye in Aqueous Media using PbS/CTAB Nanocomposites

Amanullakhan Pathan<sup>1,\*</sup>, Chetan G. Prajapati<sup>2</sup>, Riddhi P. Dave<sup>3</sup> and C. P. Bhasin<sup>4</sup>

<sup>1</sup>Shri Sarvajani Science College (PG), Mehsana-384001, India

<sup>2</sup>Humanities and Science Department, Government Engineering College, Palanpur-385001, India

<sup>3</sup>Central University of Gujarat, Gandhinagar-382030, India

<sup>4</sup>Department of Chemistry, Hemchandracharya North Gujarat University, Patan- 384265, India

Received: 2 Feb. 2022, Revised: 22 Mar. 2022, Accepted: 9 Apr. 2022

Published online: 1 May 2022

**Abstract:** In this Chapter, we demonstrated the synthesis of Lead sulphide by using low-cost chemical displacement method. We used thioacetamide for the source of sulphide ion and for the source metal salt; lead nitrate was used. The structural, morphological, metal percentage and optical properties of as synthesized nanoparticles are investigated by using X-ray diffraction (XRD), Uv-Visible spectra; Field emission gun Scanning electron microscopy (FEG-SEM) with EDS, Fourier transforms infrared spectroscopy (FTIR), High-resolution transmission electron microscopy (HR-TEM) and Photoluminescence spectroscopy (PL). The average particle size of the nanoparticles from the x-ray diffraction is about 20 nm and also field emission gun Scanning electron microscopy shows good morphology and exhibited clearly cubic shape. Further, the photocatalytic degradation of Janus green B dye was measured by visible absorption spectroscopy. To obtain the optimal conditions for the dye degradation, the effect of various experimental parameters, i.e., pH, amount of nanoparticles, concentration of dye and light intensity on the rate of reaction was studied. It was found that the JGB dye degradation gave the best results at a pH of 7.0, dye concentration= 200 ppm and using a  $70 \text{ mW}\cdot\text{cm}^{-2}$  light intensity with 0.5 g of PbS nanoparticles. At room temperature, the photocatalytic degradation of Janus green B dye was observed about 93.5%.

**Keywords:** Nanoparticles, Lead Sulfide, XRD, FTIR, UV-Vis, FEG-SEM, EDAX, HR-TEM.

## 1 Introduction

The properties of semiconductor nanostructured materials depend not only on their chemical composition but also on their shape and size [1,2,3,4,5,6]. Semiconductor medicine and materials science and their different interdisciplinary fields, nanocrystallines exhibit electronic, magnetic, optical, photochemical, and photo physical properties greatly differing from those observed in the corresponding bulk materials due to quantum size effects, resulting from predominant number of surface atoms in nano-scale materials [7,8]. Semiconductor nanoparticles have good optical and electronic properties and there has been much interest in the synthesis and characterization of sulphide nanoparticles [9,10,11]. The nanoparticles have wide applications in many fields such as solar cells [12], lasers [13], LED devices [14,15], detectors [16],

Telecommunication [17], optical switches and optical amplification. Transition metal chalcogenides are very important semiconductor materials, especially in nano-scale because of their excellent photoelectron transformation properties and potential application in physics, chemistry, biology, for instances solar cells, sensitive sensor, photon computer, and slow-release medicament [18]. Bulk PbS (rock salt crystal structure) is a direct band gap IV–VI semiconductor with a band gap of 0.41 eV and an exciton Bohr radius of 18 nm at room temperature, which means that an obvious quantum confinement effect can be observed in PbS nanocrystals. PbS nanocrystals can be used in electro luminescent devices such as light-emitting diodes, and optical devices such as optical switches due to the high third order nonlinear optical properties [19]. The size, shape, capping material and surface characteristics have a strong influence on the optical properties of PbS

\*Corresponding author E-mail: [amankhan255@gmail.com](mailto:amankhan255@gmail.com)

nanocrystals. Much attention has been paid to controlling these parameters to manipulate the optical properties of PbS nanocrystals. A great deal of research effort has been devoted to the methods of synthesis of PbS nanocrystals with various sizes and shapes in a controllable manner such as colloidal solution [20,21,22,23,24,25] or using strong organic [26,27,28] and inorganic [29,30,31] matrix supports to stabilize nanocrystals. In our previous report, we have used PVA as organic surface passivating agent to synthesize PbS nanoparticles, and the obtained nanostructure of cubic morphology with the size of 42–5 nm [18]. Azo dyes account for over 70% of all synthetic dyes consumed by the dyeing industry globally. One or more azo groups (-N=N-) operate as chromophores in the molecular structure of a reactive azo dye. Furthermore, molecules containing the azo group constitute the majority of synthetic dyes and are difficult to breakdown even at low concentrations due to their resistance to light, heat, chemicals, and microbial attacks. As a result, the removal of such synthetic dyes has become critical prior to the release of waste industrial effluents into the environment's water. Many attempts have been undertaken to remove dyes from wastewaters utilizing commonly used processes such as photocatalytic degradation of Rose Bengal, Congo red and Methylene blue dyes [32,33,34]. Zhou *et al.* have prepared 100 nm PbS truncated nanocubes and nanocubes by using cetyl trimethyl ammonium bromide and polyvinyl pyrrolidone (PVP) as surface passivating agents [35]. PbS nanocubes with the size of 50–80 nm has been synthesized using PVP and glycerol by Dong *et al* [36]. However, the size of PbS nanocubes was too large (50–100 nm) and thus further size reduction is required to observe the quantum confinement effect. Therefore, various physical and chemical synthesis methods have been developed to produce PbS nanocrystalline material with different sizes and shapes in a controllable manner. One of the major disadvantages of physical methods is the agglomeration of the nanoparticles. On the other hand, chemical synthesis apart from being simple and cheap process offers an easy way of preventing agglomeration of the nanoparticles. In general, during chemical synthesis of nanoparticles, a suitable organic stabilizer is added, which caps the nanoparticles and thus avoids their aggregation. Addition of organic stabilizers also improves chemical properties (stability, solubility etc.) as well as the physical properties (light emission characteristics). The surface modification by stabilizers can remove the localized surface trap states and significantly increases the quantum yield of the excitonic emission.

The present study deals with PbS Nanoparticles prepared by Displacement Method. The present method is very low cost and very easy to prepare PbS Nanoparticles. In this method, we used CTAB as a stabilizer. We used thioacetamide for the source of sulphide ion and for the source of metal salt; lead nitrate was used. Synthesized Lead Sulfide nanoparticles are characterized by various

analytical techniques like X-ray diffraction (XRD), Uv-Visible Spectra; Field emission gun scanning electron microscopy (FEG-SEM) with EDS, Fourier transforms infrared spectroscopy (FTIR), High-resolution transmission electron microscopy (HR-TEM) and Photoluminescence spectroscopy (PL). The Photocatalytic activity of synthesized PbS nanoparticles was investigated by photo degradation of Janus Green B dye.

## 2 Experimental

### 2.1 Materials

AR-grade Lead nitrate, thioacetamide, cetyl trimethyl ammonium bromide (CTAB), methanol and Janus Green B dye (JGB) were used as received from the *s.d fine* and Himedia chemicals (India). All reactions were performed using double distilled water.

### 2.2 Synthesis of PbS nanoparticles

The PbS nanoparticles were prepared by reaction of 1 mol of Pb (NO<sub>3</sub>)<sub>2</sub> and 2 mol of Thioacetamide. Lead nitrate was dissolved in 30 ml double distilled water and was a transferred to a round bottom flask. In a separate beaker 2 mol of thioacetamide and 1 mol of cetyl trimethyl ammonium bromide (CTAB) were dissolved in 50 ml of methanol. This mixture was added drop wise in metal salts solution and the resulting mixture was refluxed at around 65 °C for 2 hrs. After 2 hrs, colour of the solution changed from light green to dark black. Black solution was cooled at room temperature. The nanoparticles were centrifuged and were washed with double distilled water for 5 times to remove the impurities. For Calcination these nanoparticles were transferred to silica crucible and kept in muffle furnace at 600 °C for 2 hrs. After this process the crystalline nanoparticles of PbS were obtained.

### 2.3 Photocatalytic activities

The photocatalytic activity of the nanoparticles was assessed by monitoring decolorization of Janus Green B in the presence of visible light. Janus green B dye is cationic dye. The photocatalytic experiments were carried out in an immersion well photo reactor (consisting of inner and outer jacket) made up of Pyrex glass, equipped with water circulating jacket. Irradiations were carried out using a visible light 200 W tungsten lamp (Philips). The Reaction temperature was kept constant at 30 °C. Before irradiation experiments, 100 mL of the dye solution of appropriate concentration containing the desired quantity of the photocatalyst (0.1 to 0.6 g) and a predetermined amount of 2mM NaOH solution (For pH), was magnetically stirred, while the solution was at least 15 min in the dark to attain adsorption–desorption equilibrium between the dye solution and the catalyst surface. Afterwards, first sample (at 0min) was taken out and the irradiation was started.

During irradiation, samples of 5-10 mL were withdrawn at regular time (every 15 min) intervals, centrifuged and the

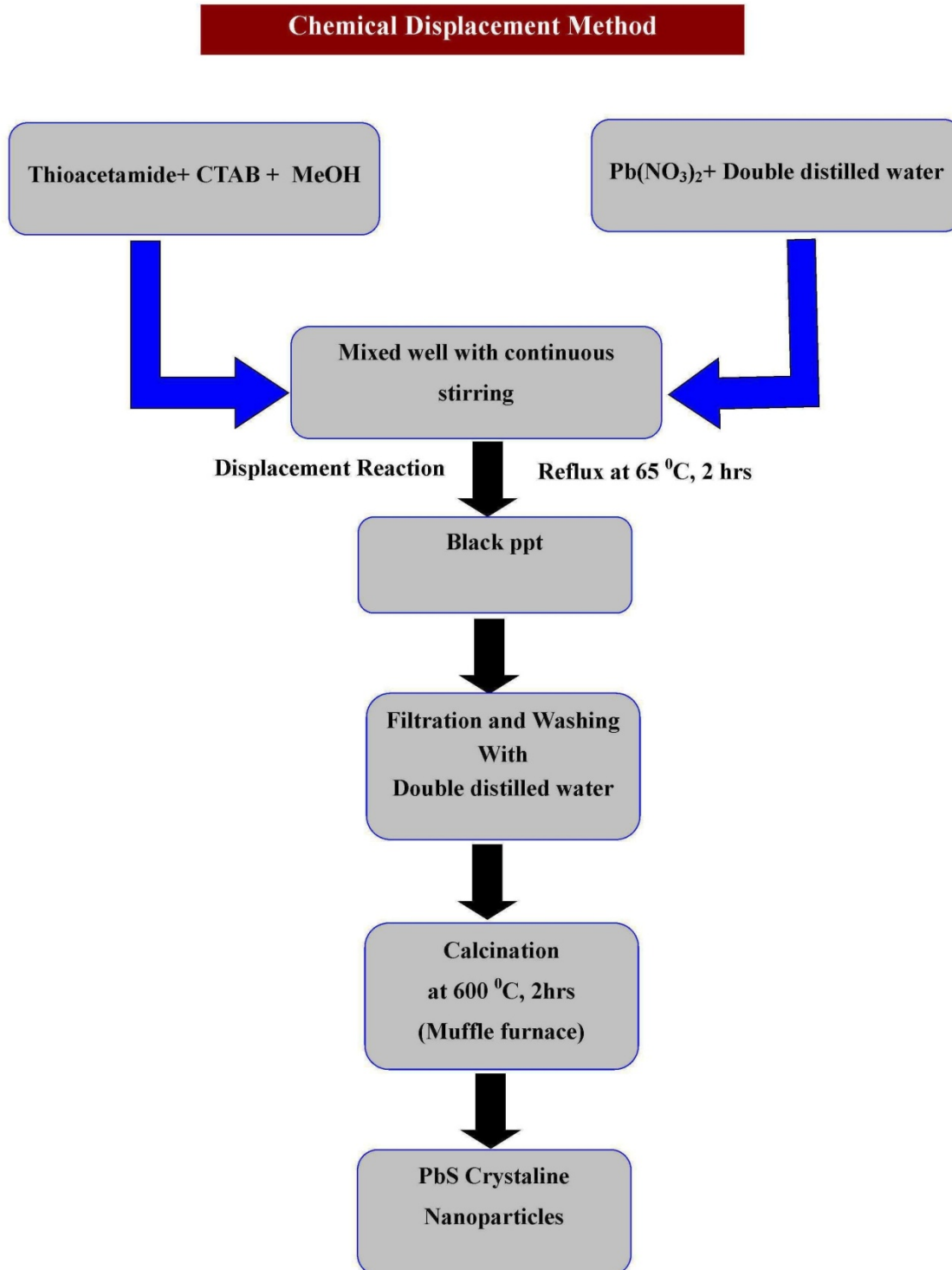


**Fig.1:** Schematic diagram for the synthesis of PbS Nanoparticles.

supernatant was subsequently analyzed. The change in absorbance of the dye aliquots was followed at its  $\lambda_{\text{max}}$  (660 nm) as a function of irradiation time. The observed absorbance spectra are in accordance with Beer-Lambert Law in the range of examined dye concentration.

The concentration of dye was calculated by standard calibration curve obtained from the absorbance of the dye at different known concentrations. The photocatalytic experiments were repeated three times in order to check the reproducibility of the experimental results. The accuracy of the optical density was found to be within  $\pm 5\%$ . The consistency in activity of the catalyst was analyzed by the recycling experiments. After the first attempt of the photocatalysis experiment, the catalyst was retrieved from the photo reactor and the aliquots by centrifugation. The retrieved catalyst was thoroughly washed with deionized water and distilled ethanol. The catalyst was dried at  $60^\circ\text{C}$  for 12h and then reused in the next cycle of the photocatalysis experiment.

Equally, the experiment was repeated for a set of cycles to monitor the loss inefficiency of the catalyst after repetitive use.

The photocatalyst amount was optimized by a series of

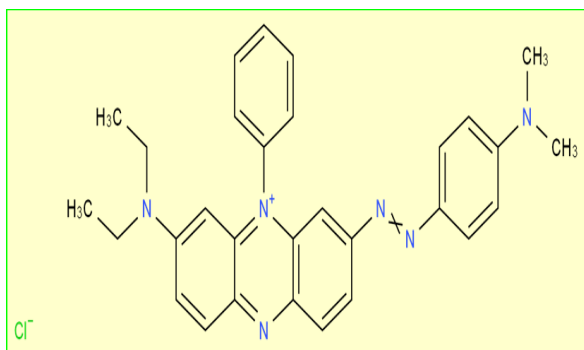


**Fig.2:** Chemical Structure of Janus Green B dye.

Photocatalysis experiments. Higher amount of photocatalyst were thought to absorb more incident photons and produce more photogenerated charge carriers, but past a particular concentration, the particles suspended in the solution cause shielding and light scattering, affecting the light transmittance in solution. Moreover, the decreasing transmittance may enhance recombination as the photons could not be continuously injected onto the photocatalyst particles. Similarly, the initial dye solution concentration has significant influence on the activity as it affects the light penetration into solution. This result was consistent with literature for the effect of initial concentration on photocatalysis.

The degradation efficiency (%) was calculated as follows:

$$\text{Degradation (\%)} = \frac{C_0 - C}{C_0} \times 100 \dots \dots \dots (1)$$

Where  $C_0$  is the initial concentration of JG, and  $C$  is the time-dependent concentration of dye upon irradiation. The following first order kinetic degradation equation can be used to describe photocatalytic JG B degradation.

$$\ln \left( \frac{C_0}{C_t} \right) = kt \dots \dots \dots (2)$$

Where  $C_0$  and  $C_t$  are the concentrations of dye in solution at times 0 and  $t$  respectively, and  $k$  is the first-order rate constant ( $\text{min}^{-1}$ ).

## 3 Results and Discussion

### 3.1 Characterization of lead sulfide nanoparticles

#### 3.1.1 Uv-Vis spectrum of PbS nanoparticles:

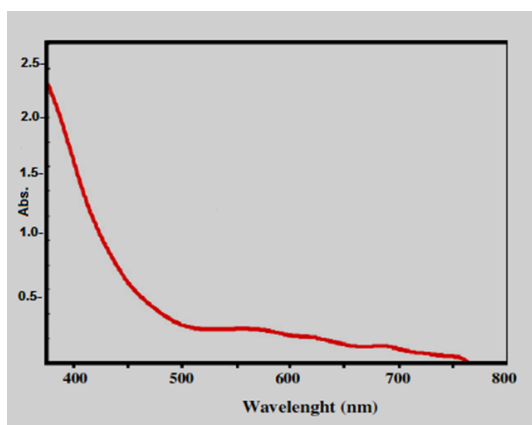


**Fig.3:** Uv-Vis absorption spectrum of synthesized PbS nanoparticles.

The Figure-3 shows that Uv-Vis absorption spectrum of synthesized PbS nanoparticles dispersed in the distilled water using by Probe sonication. The UV absorption was observed at 495 nm. This confirms the formation of lead sulfide Nanoparticles.

#### 3.1.2 FTIR spectra of PbS nanoparticles:

**Figure-4** shows the FTIR spectrum of PbS Nanoparticles. The vibrations appeared in the spectrum were in the range as reported earlier. However, the observed Peaks at  $2391$ ,  $2289 \text{ cm}^{-1}$  is due to C-H bonding. Other peaks observed mainly at  $3523 \text{ cm}^{-1}$  are due to water molecules and the peak position at  $630 \text{ cm}^{-1}$  is due to the Pb-S bending vibration mode.

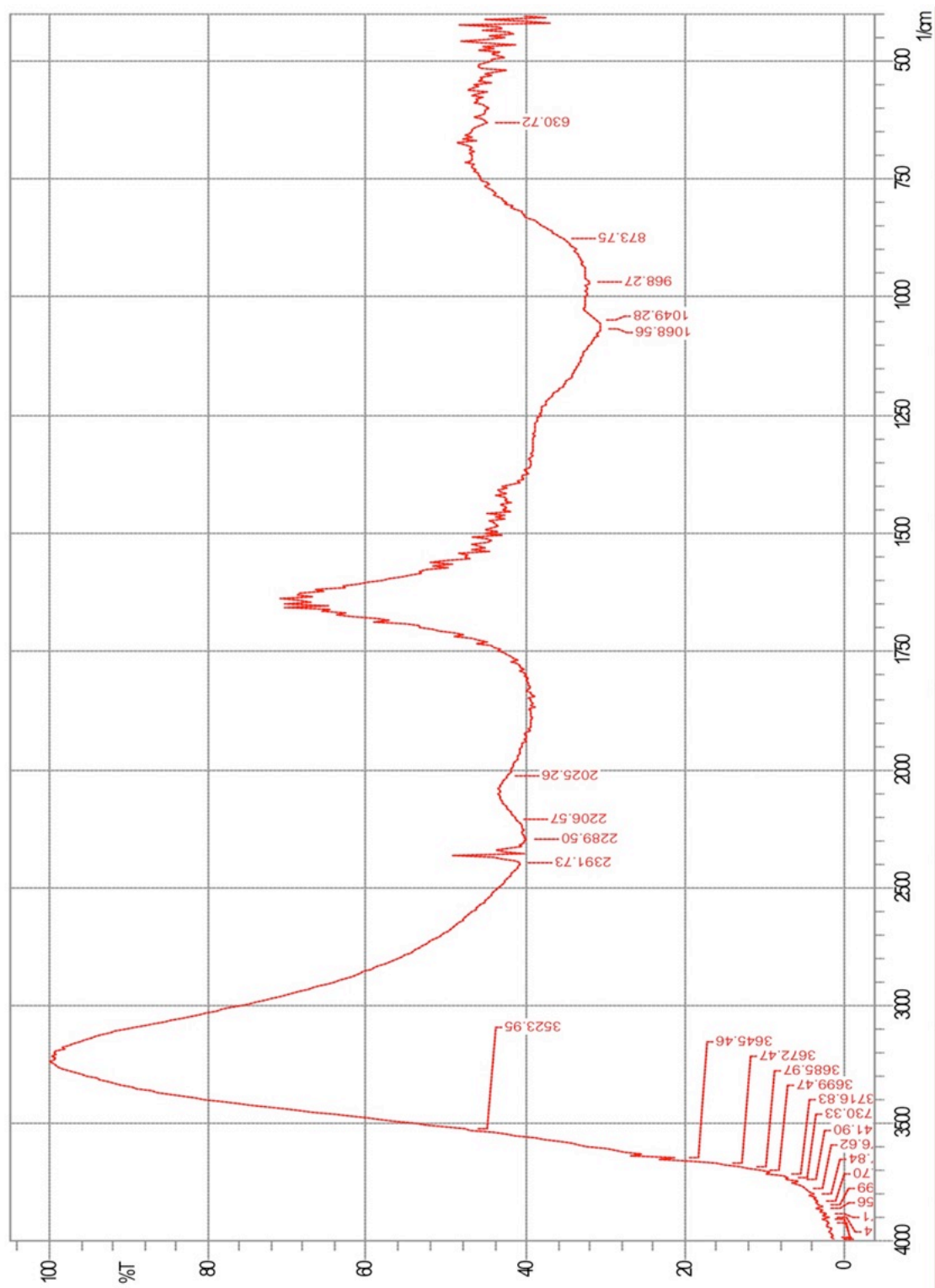


**Fig.4:** FTIR spectrum of PbS nanoparticles.

### 3.1.3 XRD spectra of PbS nanoparticles

The Lead sulfide nanoparticles synthesized by displacement process were characterized by X-ray powder diffraction (XRD) to evaluate and study their structure. XRD spectra of the synthesized Lead sulfide nanoparticles are shown in Figure-5. As seen, the obtained nanoparticles have good crystallinity. The extended peaks are representing the dimensions of the Nanoparticles. Peaks are observed at 25.920, 29.920, 42.910, 510, 53.810, 62.970, 68.810, 710 and 79.100 respectively corresponding to the (h k l) values of the peaks (1 1 1), (2 0 0), (2 2 0), (3 1 1), (2 2 2), (4 0 0), (3 1 1), (4 2 0) and (4 2 2) respectively. All the diffraction peaks in the spectra are analogous to the literature pattern of face centered cubic phase PbS (galena) powder (JCPDS file no.5-592), confirming the formation of PbS particles, which inconsistent with values reported in the previous literature [37,38]. Also, the average particle size of the PbS Nanoparticles was estimated by the Scherrer equation.

$$D = \frac{0.9\lambda}{\beta \cos\theta}$$

Where, D is the average crystalline size of the PbS nanoparticles,  $\theta$  is the peak position angle,  $\lambda$  is is wavelength of the X-ray radiation and  $\beta$  is the full width at half-maximum (FWHM) of the XRD corresponding Peaks. The results show that the average crystalline size of the obtained lead sulfide nanoparticles is 20 nm and Lattice strain 0.0044.

### 3.1.4 Field emission gun scanning electron microscope (FEG-SEM) with EDS of PbS nanoparticles

Field emission gun scanning electron microscopy (FEG-SEM) analysis was performed by JEOL JSM-7600F model and showed morphological features and examine the surface morphology and distribution of nanoparticles. The **Figure-6** shows FEG-SEM micrographs of the PbS nanoparticles presented the homogenous distribution of nano particles. FEG-SEM images (**Figure-6**) represented the spherical cluster of PbS nanoparticles. The Stoichiometric composition of PbS nanoparticles is shown in the EDS profile. From the micrograph, it was observed that the nanoparticles are almost uniform in size. The PbS Nanoparticle morphology was observed like cubic shape.

The EDS spectra obtained for PbS nanoparticles (**Figure-7**). EDS spectra of PbS show the peaks for Lead and Sulfur elements indicating the good development of PbS nanoparticles. Peak indexing of the elements is Sulfur 2.4 keV and Lead 1.8, 2.5, 2.7, 9.2 keV. The compositions in the mass percentage of the elements are Sulfur 41.34 % and Lead 46.28 %. The above data indicate no other impurities in synthesized PbS nanoparticles.

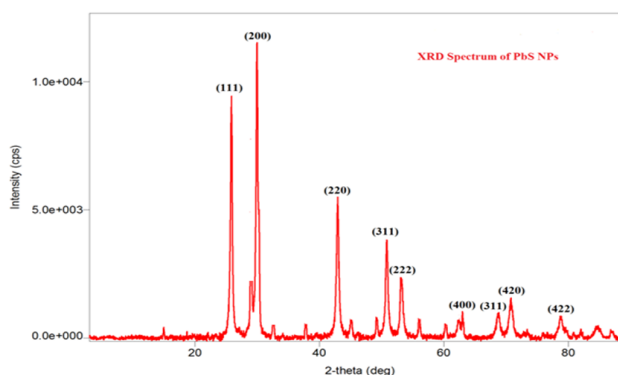


**Fig. 5** X-ray diffraction spectra of PbS nanoparticles.

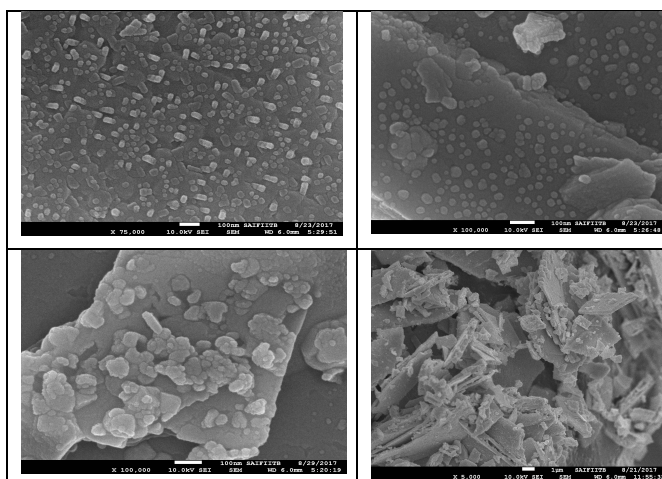


**Fig.6:** FEG-SEM images for Lead Sulfide nanoparticles.

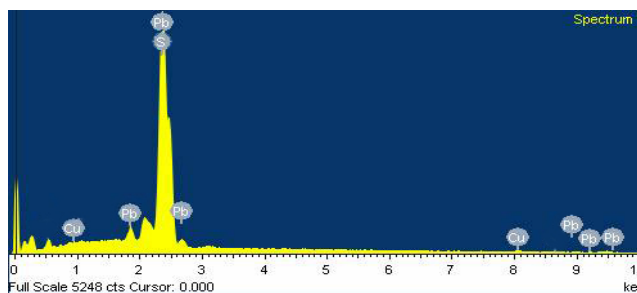


**Fig.7:** EDS spectra for Lead sulfide nanoparticles.

### 3.1.5 High resolution transmission electron microscope (HR-TEM) of PbS nanoparticles

High resolution transmission electron microscopy (HR-TEM) was performed using Tecnai G2-F30 model. Crystalline Size and shape morphology studied by HR-TEM. The HR-TEM images (**Figure-8**) confirm the particle size of the PbS is to be 25 nm in cubic shape. Using the selected area electron diffraction (SAED) pattern with bright circular spots, the crystallinity of the PbS nanoparticles was evidenced.

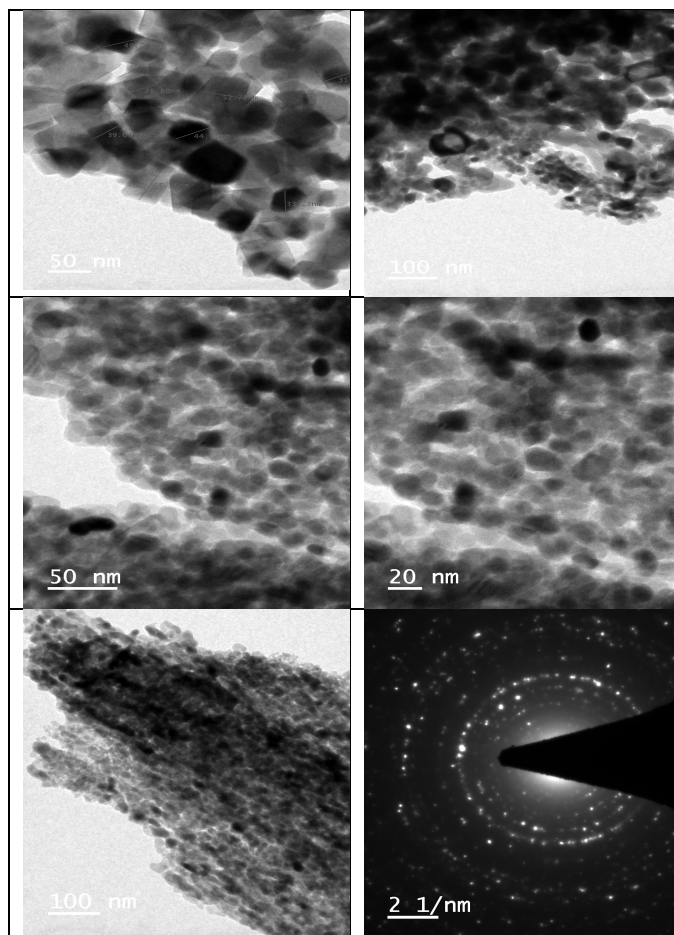


**Fig.8:** HR-TEM images for Lead sulfide nanoparticles.

### 3.1.6 Photoluminescence Spectrum of Lead Sulfide Nanoparticles

The photoluminescence spectrum of lead sulfide nanoparticles is shown in the **figure-9**. The excitation wavelength was 650 nm. The emission spectrum shows broad peaks at 792 nm. The peaks were attributed to emissions from defect levels. As observed from figure, a sharp emission peak is observed at 792 nm when the samples were excited at 650 nm. The peak position remains constant in all the cases, although a variation in intensity has been founded. M. Navaneethan *et al.* have reported an emission at 796 nm in the PL spectra of PbS on excitation at 760 [38].

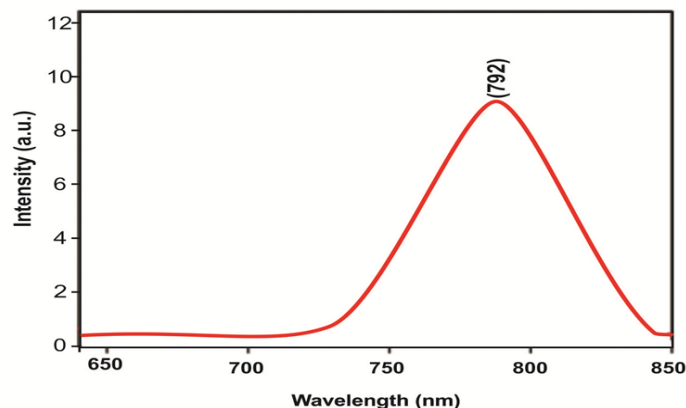


**Fig.9:** Photoluminescence spectra of lead sulphide nanoparticles.

### 3.2 Photocatalytic activities:

The photocatalytic degradation of Janus Green B dye using PbS nanoparticles under visible light was investigated by visible absorption spectroscopy, and most kinetic measurements were performed at room temperature (300 K). The concentration of dye in the form of absorbance before and after photocatalytic degradation was measured at 660 nm ( $\lambda_{\text{max}}$  value obtained for Janus Green B dye). A 200 W tungsten lamp (Philips) was used as the visible light source. A cutoff filter was placed between the light and the sample (filled with water) to remove the thermal radiation just to ensure elucidation by visible light. The progress of the photocatalytic reaction was observed by taking absorbance at regular time intervals.

#### 3.2.1 Effect of the amount of PbS nanoparticles

The effects of the amount of PbS nanoparticles are also likely to affect the process of dye degradation and therefore, different amounts of nanoparticles were used.

It has been observed that as the amount of nanoparticles was increased, the rate of photo degradation of Janus Green B also increased as well as the number of active sites. But ultimately the rate became almost constant after adding a certain amount (0.5 g) of nanoparticles. This may be due to the fact that, after a certain limit, the increase in amount of PbS nanoparticles did not increase the exposed surface area (active sites) of the nanoparticles. It only increased the thickness of the layer, as the bottom of the reaction vessel was covered by the nanoparticles. It may be considered that a kind of saturation point was reached, and that, after this saturation point no effect of amount of nanoparticles was observed. This hypothesis was also confirmed by using reaction vessels of different dimensions. As the bottom area of the vessel increased, the nanoparticles exposed area also increased, hence, the rate of photocatalytic degradation increased. In the present work, beakers of the same size were also used for a whole experiment and, after a

maximum exposure to nanoparticles; further addition of nanoparticles only increased the layer thickness, but did not contribute to increase the photocatalytic degradation rate.

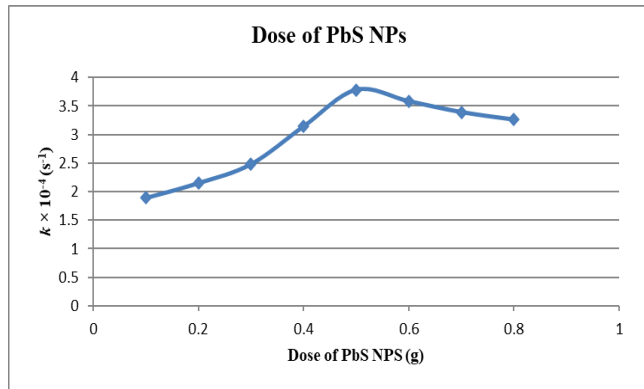


**Fig.10:** Effective dose of PbS nanoparticles.

### 3.2.2 Effect of pH

The effect of pH on photocatalytic degradation was investigated in the range 4.5 – 8.

It is evident from the data that the degradation rate of Janus Green B increases with increasing pH of solution up to 7 and above this value of pH, the rate of photocatalytic degradation of Janus Green B starts decreasing. It may be explained on the basis that at low pH, the azo dye (Figure 2) was attracted by positively charged surface of nanoparticles, but after a certain limit, further increase in pH turned surface of nanoparticles as negatively charged. Due to presence of lone pairs on two oxygen atoms, Janus Green B (Figure 2) seems to face a force of repulsion from negatively charged surface of the nanoparticles, which results into a decreasing rate of reaction.

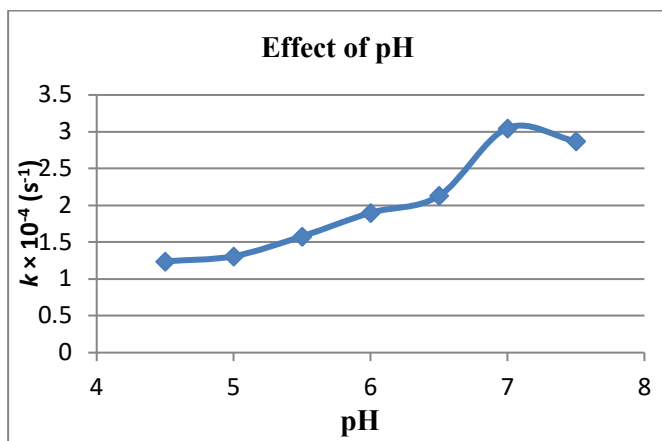


**Fig.11:** Effect of pH.

### 3.2.3 Effect of concentration of Janus Green B dye

The concentration of dye was varied from 50 ppm to 250 ppm.

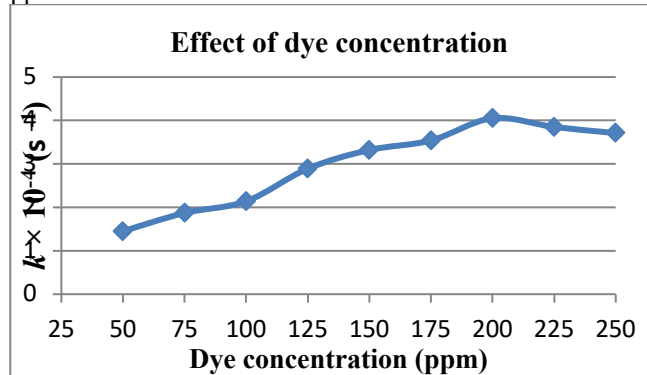


**Fig.12:** Effect of Dye concentration.

It has been observed that the rate of photocatalytic degradation increases with increase in the concentration of the dye up to 200 ppm. This may be due to the fact that as the concentration of the Janus Green B was increased, more dye molecules were available for excitation and consecutive degradation. Hence, an increase in the rate was observed. The rate of photocatalytic degradation was found to decrease with further increase in the concentration of dye. This may be attributed to the fact that the dye started acting as a filter for the incident light and it does not permit the desired light intensity to reach the photocatalyst surface in a limited time domain; thus, decreasing the rate of photocatalytic degradation of Janus Green B.

### 3.2.4 Effect of light intensity

The effect of the variation of the light intensity on the rate was also investigated and the observations are represented in graph.

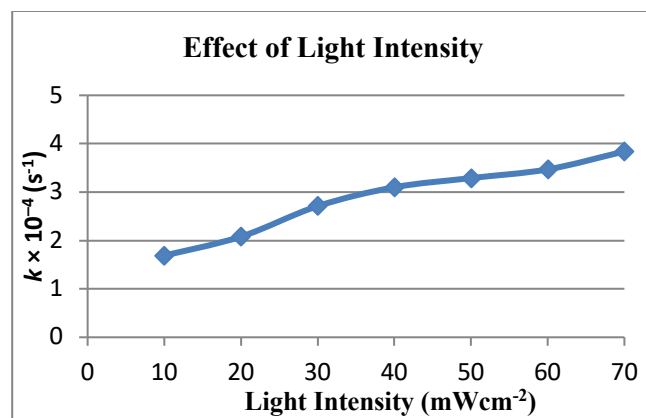
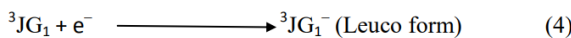
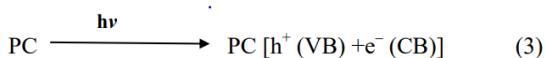
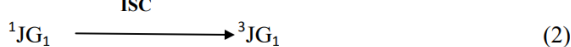
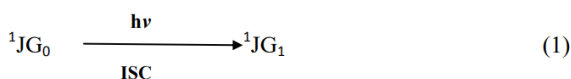


**Fig.13** Effect of Light intensity

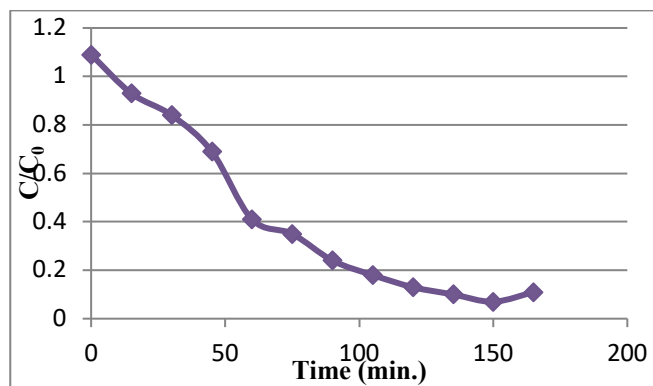
The data indicate that the degradation action was accelerated as the intensity of light was increased, because any increase in the light intensity increases the number of photons striking per unit time per unit area of the nanoparticles. An almost linear behavior between light intensity and the rate of reaction has been observed. However, higher intensities were avoided due to thermal effects.

### 3.2.5 Tentative mechanism of Janus Green B photo degradation

On the basis of our experimental observations, a tentative mechanism for photocatalytic degradation (mineralization) of Janus Green B may be proposed as:



In the reaction, dye molecules absorb radiations of suitable wavelength and give rise to the singlet excited state (1). Then it may undergo an intersystem crossing (ISC) process to yield the more stable triplet excited state of the dye (2). Photo catalyst (PbS NPS) (PC) also utilizes the radiant energy to excite its electron from the valence band (VB) to the conduction band (CB), thus, leaving behind a hole ( $h^+$ ) in the VB (3). The electron present in the CB may be utilized to reduce the dye triplet excited state into its Leuco form (4), which ultimately degrades to photoproducts (5). Another possible variant of this tentative mechanism would be the reduction of the dye excited singlet state ( ${}^1JG_1$ ). The absence of role of hydroxyl radicals in this photocatalytic reaction was also confirmed by the fact that the reaction rate remained almost unaffected in the presence of the hydroxyl radical scavenger, 2-propanol.



Janus Green B dye = 200 ppm; PbS NPs = 0.5 g,  
Light intensity = 70 mWcm<sup>-2</sup>; pH = 7, R.T.

Fig.14: Photocatalytic performance of PbS nanoparticles.

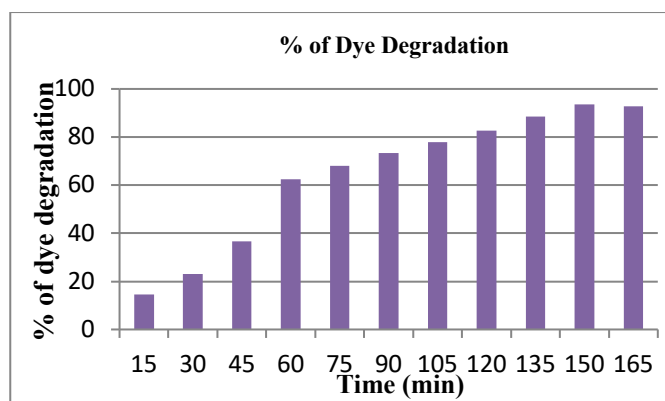


Fig.15: Photocatalytic degradation of Janus Green B dye.

## 4 Conclusions

Lead sulfide nanoparticles were successfully prepared by the use of Low cost and very effective chemical Displacement reaction at optimum conditions with using CTAB as a stabilizer. Synthesized lead sulfide nanoparticles by the chemical displacement method were composed of the Cubic in shape. The composition and structure of the synthesized Lead sulfide nanoparticles at optimum conditions were characterized by UV-Vis, FT-IR, XRD, FEG-SEM, EDS, HR-TEM and PL (photoluminescence) techniques. The results of present study clearly confirmed the formation of Lead sulfide nanoparticles. From UV-Vis spectra, absorption peak observed around 495 nm confirms the formation of PbS NPs and XRD patterns show that average particles size found 20 nm. Photocatalytic activity of the prepared PbS nanoparticles was studied and the results exposed the potential of the synthesized lead sulfide nanoparticles as a photo catalyst in Janus Green B (JGB) dye degradation. The degradation rate increased with increasing pH because more hydroxyl ions were present (generating more hydroxyl radicals). It attains maximum rate at pH 7.0; a

further increase in pH above 7.0 results in a decrease in the rate of the reaction, because of decreasing attraction between the neutral form of the dye and the negatively charged nanoparticles surface. Increasing the concentration of Janus Green B also increased the rate up to a certain value due to the increase in the number of dye molecules, but it shows a declining behavior on further increase of the concentration of dye. This decrease may be attributed to the fact that at higher concentration, the dye may act as an internal filter for the incident radiations, which decreases the intensity of the incident radiation on the nanoparticles. The results indicate that initially the rate increases with increasing amount of nanoparticles but after 0.5 g, the rate becomes virtually constant (saturation behavior). This may be due to the complete coverage of the bottom of the reaction vessel by the nanoparticles. Any further increase will not add to an increase in the exposed surface area but only increases the thickness of the layer. An increase in the light intensity will increase the number of photons striking Lead sulphide nanoparticles per unit area per second and as a consequence, the reaction rate increases almost linearly with the increase in light intensity. Scavengers trap the active species by reducing their activity in the solution and as a result reaction rate becomes quite low or reaction almost stops. The optimum reaction conditions were obtained as: pH = 7.0; [Janus Green B] = 200 ppm; PbS NPs = 0.5 g; contact time = 150 min; light intensity = 70.0 mWcm<sup>-2</sup>. The results showed after optimum reaction conditions maximum degradation (about 93.5 %) of JG-B was achieved.

## References

- [1] Hammad, Talaat M., Jamil K. Salem, and Roger G. Harrison. "Synthesis, characterization, and optical properties of Y-doped ZnO nanoparticles." *Nano.*, **4(4)**, 225-232, (2009).
- [2] Hammad, Talaat M., Jamil K. Salem, and Roger G. Harrison. "The influence of annealing temperature on the structure, morphologies and optical properties of ZnO nanoparticles." *Superlattices and Microstructures.*, **47(2)**, 335-340, (2010).
- [3] Hammad, Talaat M., and Jamil K. Salem. "Synthesis and characterization of Mg-doped ZnO hollow spheres." *Journal of Nanoparticle Research.*, **13(5)**, 2205-2212, (2011).
- [4] Salem, Jamil K., Talaat M. Hammad, and Roger R. Harrison. "Synthesis, structural and optical properties of Ni-doped ZnO micro-spheres." *Journal of Materials Science: Materials in Electronics.*, **24(5)**, 1670-1676, (2013).
- [5] Salem, Jamil K., Talaat M. Hammad, S. Kuhn, Mohammed Abu Draaz, Naser K. Hejazy, and R. Hempelmann. "Structural and optical properties of Co-doped ZnS nanoparticles synthesized by a capping agent." *Journal of Materials Science: Materials in Electronics.*, **25(5)**, 2177-2182, (2014).
- [6] Salem, Jamil K., Talaat M. Hammad, S. Kuhn, Issa Nahal, Mohammed Abu Draaz, Naser K. Hejazy, and R. Hempelmann. "Luminescence properties of Mn and Ni doped ZnS nanoparticles synthesized by capping agent." *Journal of Materials Science: Materials in Electronics.*, **25(12)**, 5188-5194, (2014).
- [7] Hammad, Talaat M., Jamil K. Salem, S. Kuhn, Mohammed Abu Draaz, R. Hempelmann, and Fawzi S. Kodeh. "Optical properties of Cu<sup>2+</sup> and Fe<sup>2+</sup> doped ZnS semiconductor nanoparticles synthesized by co-precipitation method." *Journal of Materials Science: Materials in Electronics.*, **26(7)**, 5495-5501, (2015).
- [8] Hancock, Jared M., William M. Rankin, Talaat M. Hammad, Jamil S. Salem, Karine Chesnel, and Roger G. Harrison. "Optical and magnetic properties of ZnO nanoparticles doped with Co, Ni and Mn and synthesized at low temperature." *Journal of nanoscience and nanotechnology.*, **15(5)**, 3809-3815, (2015).
- [9] Zhu, Junjie, Suwen Liu, O. Palchik, Yuri Kolytyn, and A. Gedanken. "A novel sonochemical method for the preparation of nanophasic sulfides: synthesis of HgS and PbS nanoparticles." *Journal of Solid State Chemistry.*, **153(2)**, 342-348, (2000).
- [10] Kruis, Frank Einar, Heinz Fissan, and Bernd Rellinghaus. "Sintering and evaporation characteristics of gas-phase synthesis of size-selected PbS nanoparticles." *Materials Science and Engineering: B* **69**, 329-334, (2000).
- [11] Kruis, F. Einar, Heinz Fissan, and Aaron Peled. "Synthesis of nanoparticles in the gas phase for electronic, optical and magnetic applications—a review." *Journal of Aerosol Science.*, **29(5)**, 511-535, (1998).
- [12] Günes, Serap, Karolina P. Fritz, Helmut Neugebauer, Niyazi Serdar Sariciftci, Sandeep Kumar, and Gregory D. Scholes. "Hybrid solar cells using PbS nanoparticles." *Solar Energy Materials and Solar Cells.*, **91(5)**, 420-423, (2007).
- [13] Guerreiro, P. T., S. Ten, N. F. Borrelli, J. Butty, G. E. Jabbour, and N. Peyghambarian. "PbS quantum-dot doped glasses as saturable absorbers for mode locking of a Cr: forsterite laser." *Applied Physics Letters.*, **71(12)**, 1595-1597, (1997).
- [14] Hines, Margaret A., and Gregory D. Scholes. "Colloidal PbS nanocrystals with size-tunable near-infrared emission: observation of post-synthesis self-narrowing of the particle size distribution." *Advanced Materials.*, **15(21)**, 1844-1849, (2003).
- [14] Zhao, Xusheng, Ivan Gorelikov, Sergei Musikhin, Sam Cauchi, Vlad Sukhovatkin, Edward H. Sargent, and Eugenia Kumacheva. "Synthesis and optical properties of thiol-stabilized PbS nanocrystals." *Langmuir.*, **21(3)**, 1086-1090, (2005).
- [15] Kumar, Anil, and Anshuman Jakhmola. "Photophysics and charge dynamics of Q-PbS based mixed ZnS/PbS and PbS/ZnS semiconductor nanoparticles." *Journal of colloid and interface science.*, **297(2)**, 607-617, (2006).
- [16] H Sargent, E. "Infrared quantum dots." *Advanced Materials* **17(5)**, 515-522, (2005).
- [17] Hammad, Talaat M., Jamil K. Salem, S. Kuhn, Nadia M. Abu Shanab, and R. Hempelmann. "Surface morphology

- and optical properties of PVA/PbS nanoparticles." *Journal of Luminescence.*, **157**, 88-92, (2015).
- [18] Kane, R. S., R. E. Cohen, and R. Silbey. "Theoretical study of the electronic structure of PbS nanoclusters." *The Journal of Physical Chemistry.*, **100(19)**, 7928-7932, (1996).
- [19] Eychmüller, A., A. Hässelbarth, L. Katsikas, and H. Weller. "Photochemistry of Semiconductor Colloids. 36. Fluorescence Investigations on the Nature of Electron and Hole Traps in Q-Sized Colloidal CdS Particles." *Berichte der Bunsengesellschaft für physikalische Chemie.*, **95(1)**, 79-84, (1991).
- [20] Lu, S. W., Ulrich Sohling, Martin Mennig, and H. Schmidt. "Nonlinear optical properties of lead sulfide nanocrystals in polymeric coatings." *Nanotechnology.*, **13(5)**, 669-673, (2002).
- [21] Rossetti, R., R. Hull, J. M. Gibson, and L. E. Brus. "Hybrid electronic properties between the molecular and solid-state limits: lead sulfide and silver halide crystallites." *The Journal of chemical physics.*, **83(3)**, 1406-1410, (1985).
- [22] Wang, Ying, and N Herron. "Nanometer-sized semiconductor clusters: materials synthesis, quantum size effects, and photophysical properties." *The Journal of Physical Chemistry.*, **95(2)**, 525-532, (1991).
- [23] Nenadovic, M. T., T. Rajh, and O. I. Micic. "Size quantization in small semiconductor particles." *The Journal of Physical Chemistry.*, **89(3)**, 397-399, (1985).
- [24] Wang, C., W. X. Zhang, X. F. Qian, X. M. Zhang, Y. Xie, and Y. T. Qian. "A room temperature chemical route to nanocrystalline PbS semiconductor." *Materials Letters.*, **40(6)**, 255-258, (1999).
- [25] Wang, Ying. "Nonlinear optical properties of nanometer-sized semiconductor clusters." *Accounts of Chemical Research.*, **24(5)**, 133-139, (1991).
- [26] Kane, R. S., R. E. Cohen, and R. Silbey. "Synthesis of PbS nanoclusters within block copolymer nanoreactors." *Chemistry of Materials* **8(8)**, 1919-1924, (1996).
- [27] Borrelli, N. F., and D. W. Smith. "Quantum confinement of PbS microcrystals in glass." *Journal of non-crystalline solids* **180(1)**, 25-31, (1994).
- [28] Salata, Oleg V., Peter J. Dobson, Peter J. Hull, and John L. Hutchison. "Fabrication of PbS nanoparticles embedded in a polymer Film by a gas-aerosol reactive electrostatic deposition technique." *Advanced Materials* **6(10)**, 772-775, (1994).
- [29] Parvathy, N. N., G. M. Pajonk, and A. Venkateswara Rao. "Synthesis and study of quantum size effect, XRD and IR spectral properties of PbS nanocrystals doped in SiO<sub>2</sub> xerogel matrix." *Journal of crystal growth* **179(1)**, 249-257, (1997).
- [30] Fendler, Janos H. "Atomic and molecular clusters in membrane mimetic chemistry." *Chemical Reviews* **87(5)**, 877-899, (1987).
- [30] Zhou, Guangjun, Mengkai Lü, Zhiliang Xiu, Shufen Wang, Haiping Zhang, Yuanyuan Zhou, and Shumei Wang. "Controlled synthesis of high-quality PbS star-shaped dendrites, multipods, truncated nanocubes, and nanocubes and their shape evolution process." *The Journal of Physical Chemistry B.*, **110(13)**, 6543-6548, (2006).
- [31] Dong, Lihong, Ying Chu, Yujiang Zhuo, and Wei Zhang. "Two-minute synthesis of PbS nanocubes with high yield and good dispersibility at room temperature." *Nanotechnology.*, **20(12)**, 125301-125302, (2009).
- [32] Pathan, A. A., Desai, K. R., & Bhasin, C. P. "Improved Photocatalytic Properties of NiS Nanocomposites Prepared by Displacement Method for Removal of Rose Bengal Dye". *Current Nanomaterials*, **2(3)**, 169-176, (2017).
- [33] Desai, K. R., Pathan, A. A., & Bhasin, C. P. "Synthesis, characterization of cadmium sulphide nanoparticles and its application as photocatalytic degradation of congo red". *Int J Nanomater Chem*, **3**, 39, (2017).
- [34] Pathan, A. A., Bhatt, S., Vajapara, S. & Bhasin, C. P. "Solar Light Induced Photo Catalytic Properties of  $\alpha$ -Fe<sub>2</sub>O<sub>3</sub> Nanoparticles for Degradation of Methylene Blue Dye". *Int. J. Thin.Film. Sci. Tec.* **9(2)**, 119-124, (2020)
- [35] Liang, Dadong, Shanshan Tang, Jianbo Liu, Jinghua Liu, Xiaoli Lv, and Lijuan Kang. "Large scale hydrothermal synthesis of PbS nanorods." *Materials letters.*, **62(16)**, 2426-2429, (2008).
- [36] Liu, Jincheng, Huangzhong Yu, Zhonglian Wu, Wenli Wang, Junbiao Peng, and Yong Cao. "Size-tunable near-infrared PbS nanoparticles synthesized from lead carboxylate and sulfur with oleylamine as stabilizer." *Nanotechnology.*, **19(34)**, 345602-345603, (2008).
- [37] Lee, S-M., S-N. Cho, and Jinwoo Cheon. "Anisotropic shape control of colloidal inorganic nanocrystals." *Advanced Materials* **15(5)**, 441-444, (2003).
- [38] Navaneethan, M., K. D. Nisha, S. Ponnusamy, and C. Muthamizhchelvan. "Optical and surface morphological properties of triethylamine passivated lead sulphide nanoparticles." *Materials Chemistry and Physics.*, **117(2)**, 443-447, (2009).